AIAA-89-1893

Transition Flight Experiments on a Swept Wing With Suction

D. V. Maddalon
NASA Langley Research Center

F. S. Collier, Jr.
High Technology Corporation

L. C. Montoya
NASA Dryden Flight research Facility

C. K. Land
NASA Langley Research Center

AIAA 20th Fluid Dynamics, Plasma Dynamics
and Lasers Conference
Buffalo, New York, June 12-14, 1989

TRANSITION FLIGHT EXPERIMENTS ON A SWEPT WING WITH SUCTION

D. V. Maddalon†, F. S. Collier, Jr.‡, L. C. Montoya*, and C. K. Land†

Abstract

Flight experiments were conducted on a 30 degree swept wing with a perforated leading edge by systematically varying the location and amount of suction over a range of Mach number and Reynolds number. Suction was varied chordwise ahead of the front spar from either the front or rear direction by sealing spanwise perforated strips. Transition from laminar to turbulent flow was due to leading edge turbulence contamination or crossflow disturbance growth and/or Tollmien-Schlichting disturbance growth- depending on the test configuration, flight condition, and suction location. A state-of-the-art linear stability theory which accounts for body and streamline curvature and compressibility was used to study the boundary layer stability as suction location and magnitude varied. N-factor correlations with transition location were made for various suction configurations.

Nomenclature

ALT	Altitude, feet
C	Chord
C_p, CP	Pressure coefficient
C_q, CQ	Suction coefficient
F	Frequency
HLFC	Hybrid Laminar Flow Control
K	Non-dimensional suction velocity
LE	Leading Edge
LEFT	Leading Edge Flight Test
LFC	Laminar Flow Control
M	Freestream Mach number
N	N-factor, where $N = \ln(A/A_0)$
NLF	Natural Laminar Flow
r	Leading edge radius (normal)
R/ft	Freestream unit Reynolds number
R_T	Transition Reynolds number based on freestream conditions
R_{cf}	Crossflow Reynolds number based on W_{max} and $D_{0.01}$
R_θ	Reynolds number based on momentum thickness of the attachment line boundary layer
S/C	Distance measured along surface, streamwise
t	Time
t/c	Thickness ratio (normal)
W	Crossflow velocity
WS	Wing station, inches
X/C	Distance measured along chord, streamwise
$D_{0.01}$	Distance from wall above W_{max} where $W = 0.01 \times W_{max}$

Greek

θ	momentum thickness
μ	Laminar coefficient of viscosity
λ	Sweep angle, degrees
μa	microamperes

Subscripts

$a.l.$	at the attachment line
CF	crossflow
max	maximum
TS	Tollmien-Schlichting
T	at transition

Introduction

The achievement of laminar flow on lifting surfaces at the Reynolds numbers and sweep angles typical of modern, high subsonic-speed, commercial transports is a formidable task. For leading edge sweep angles above approximately 15 degrees, transition may occur very near the leading edge due to the uncontrolled growth of crossflow disturbances in the laminar boundary layer. In addition, attachment line contamination from the

† LFCPO/FAD , NASA LaRC.
‡ High Technology Corp. Member AIAA
* OFA, NASA DFRF

turbulent fuselage can dash the possibility of achieving any laminar flow. Leading-edge suction is an effective method of controlling the growth of these disturbances, and combined with a 'tailored' pressure gradient over the wing box to control Tollmien-Schlichting (TS) disturbance growth, may result in extensive amounts of laminar flow (hybrid laminar-flow control, HLFC). The leading edge region of a laminar flow wing presents difficult problems associated with the attainment of laminar flow. The leading edge is subject to foreign object damage, insect impingement, rain erosion, icing and other contaminents. Anti-icing, anti-contamination, suction and perhaps purge systems must all be packaged into a relatively small leading edge box. Most of these problems are common to the laminar flow control aircraft concepts under consideration for the achievement of extensive laminar flow on aircraft wings. Data is needed to establish the practicality of this technology for laminar flow aircraft.

To provide such data, NASA completed the Leading Edge Flight Test (LEFT) Program as a flight validation of LFC leading edge systems that were being developed by NASA and U.S. airframe manufacturers. During this program, a complete perforated laminar flow control (LFC) leading edge system was installed and tested in the right wing of a Jetstar aircraft to gain operational experience from which the concept's practicality could be assessed (see figure 1). References 1 through 6 provide a detailed description of this program. At the end of the LEFT program, this aircraft performed a series of transition research experiments, the first of which are described in this paper. These experiments were designed to assess the sensitivity of transition to suction in the leading edge region, and were completed between June 1986 and April 1987. This work thus resulted in the first laminar flow flight research experiments made on a swept wing with suction boundary layer control since the X-21 LFC program ended in 1965.

Experimental Apparatus

Suction System

A schematic of the aircraft suction system as modified for the research program is presented in figure 2. The centrifugal air turbine used as a suction pump is an AiResearch turbocompressor designed for the Boeing 707 air-conditioning system and modified for this application. The compressor was located in the unpressurized rear fuselage compartment. Suction air was ducted through fifteen spanwise suction flutes beneath the perforated wing surface (figure 3). Flute air flow is individually controlled from the aircraft cabin with adjustable sonic needle valves (ref. 7). Valve control and data acquisition is accomplished at the operator station in the cabin (see figure 2).

Laminar Flow Control Test Article Description

A detailed description of the perforated leading edge is provided in reference 1. The leading edge included all the systems necessary to provide all functions required for an LFC aircraft. The leading edge sandwich panel structure was supported by ribs attached to the front spar (figure 3). Suction panel location on the wing is given in figure 4. The outer face of the suction surface panel was a titanium sheet 0.025 inch thick and perforated with over 1 million holes of 0.0025 inch diameter (drilled by an electron beam) spaced about 0.035 inch between centers. The panel core and inner face sheet were fiberglass. The panel was corrugated to form flutes for the subsurface suction air collection. Bond areas between the perforated surface and the flute core were impervious to flow. Thus, suction on the surface was along spanwise perforated strips of about 0.65 inch chord separated by non-suction strips of about 0.35 inch chord. Suction was applied to the upper surface from just below the leading edge highlight to the front spar joint (X/C = 13 percent). No attempt was made to achieve laminar flow beyond the front spar.

The perforated leading edge housed a Kruegger-type device that deployed to provide the test surface with line-of-sight protection against insect impacts during takeoff and landing. The test article was installed in the leading edge opening created by removal of auxiliary fuel tanks on the basic wing. The planform of the modified wing (figure 4) spanned about 7 feet with the suction article about 5 feet in span. Outboard and inboard, the sweep of the basic JetStar wing is 33 degrees; the test article was swept 30 degrees. At the approximate test article midspan location (WS= 165.2), the normal chord is about 9.8 feet and the normal nose radius is 1.69 inches.

To produce the desired pressure distribution, the wing section required extensive modification. Wing contour–to the rear spar on the upper surface and to the front spar on the lower surface–was changed with the installation of the test article and fiberglass fairings over the wing box and at the test article edges. The gloved wing was significantly thicker than the basic Jetstar wing, particularly in the outboard glove region. This resulted in a test article dimensionally about equivalent to the leading edge box of a DC-9-30 at the mean aerodynamic chord. The volume of the leading edge available for the laminar flow control system was thus representative of a small commercial transport.

Figure 5 shows the installed perforated test article. The white areas inboard and outboard of the test article are aerodynamic fairings to contour the test article back

into the JetStar wing surface. Aft of the front spar, a fairing extends to the rear spar to close out the wing sections.

Instrumentation

Figure 5 also shows a row of Pitot tubes near the surface at the front spar, as well as Pitot tubes used to measure the airstream reference pressure over the wing and outside the boundary layer. A closeup of these Pitots is shown in figure 6. The near surface Pitots are used to determine if laminar flow exists at the front spar, and to locate the approximate transition location ahead of each Pitot. A detailed description of the procedure used is given in ref. 3 . Probes were flight calibrated for transition location by placing three-dimensional roughness transition strips at known locations on the test surface. Boundary layer state (laminar or turbulent) was measured about every three inches over a five foot span at the front spar. The location of all instrumentation used on the test article is given in figure 7. Hot film sensors were not used in these tests. Measurements of surface pressures, duct pressures, surface and reference Pitot pressures, and other system and flight parameters were displayed at the cabin control console.

Figure 8 shows the modified aircraft in flight. The pylon on the fuselage was used as a mounting for a Knollenberg probe to measure ice particle size and count during ice cloud penetrations. The pylon also housed a charging patch for measurement of charge build up during cloud encounters (ref. 3). A charging patch reading of +0.025 to -0.050 microampere indicates clean air (ref. 3).

Experiment Description

Experiments were conducted at test conditions which included nominal Mach numbers of 0.70, 0.75, and 0.775 and altitudes of 29000, 31000, 33000, 35000 and 37000 feet. From this extensive data base, specific test points were selected for analysis, with most analysis done at 0.775 Mach and 29000 feet. For simplicity, combinations of flight conditions are referred to with the Mach number stated first and then the altitude; that is, 0.775 Mach and 29000 feet is denoted as 0.775/29000. Unit Reynolds numbers per foot varied from 1.56 x 10E6 to 2.50 x 10E6. At most test conditions, the test-article chordwise pressure gradient was nearly flat beyond $X/C = 0.05$.

Figure 9 provides the measured chordwise pressure distribution at the 0.775/29000 test condition selected for detailed analysis. The test article's measured spanwise gradient in pressure coefficient at 0.775/29000 is approximately 0.033 per foot, becoming more negative in the inboard direction. Actual midspan flute centerline locations for X/C and S/C are given in Table 1. Suction flute locations (beginning and end) used in the stability calculations at the midspan of the test article are given in Table 2. Research parameters included variations of the location and amount of suction. Suction was varied chordwise by progressively sealing spanwise perforated strips from either the front or rear direction.

Experimental Results

Spanwise Turbulence Contamination

The problem of spanwise turbulence contamination has been studied extensively in Refs. 8-14. Reference 6 described the spanwise turbulence contamination encountered during initial flight testing and its alleviation by use of a 'Gaster' bump (ref. 12). The more recent detailed data, however, is presented in figure 10 as the laminar flow area achieved on the test article planform including 'bump off' and 'bump on' results, together with the measured nominal suction level within the perforated area. The leading edge has the highest measured suction coefficient (C_q = -0.000706 in the perforated region–see Table 2) and the test-article mid-chord region has the lowest (C_q = -0.000080). For comparison purposes, the measured suction coefficient averaged over the entire perforated area is inset in the C_q figures; in figure 10, it varies from C_q = -0.000389 to -0.000349. The seven numbers included in the legend next to the test article planform specify, respectively,

Flight number
Time of day
Mach number
Altitude
Unit Reynolds number per foot
Charging patch reading in microamperes
Average transition location (% chord)

Note that when the average transition location is given as 13.0, the test article is entirely laminar.

Figure 10 presents bump off (planforms 1 and 2) and bump on (planforms 4 and 5) data at two test conditions. In referring to these figures, a shortened notation will be used. For example, planform 2 of this figure will be called figure 10-2. With the bump on, laminar flow is obtained to the front spar at both unit Reynolds numbers (fig. 10-4 and 5). With the bump off and with nominal suction, the test article is only partially laminar (fig. 10-1 and 2) at both unit Reynolds numbers, although more laminar flow is obtained spanwise at the lowest unit Reynolds number (fig. 10-1). Values of the attachment line momentum thickness Reynolds number indicate that the critical value of about 90 to 100 (ref. 10) is exceeded (fig. 11) for the 0.775/29000 flight condition; movement of the transition front (fig. 10-2 and 1) is consistent with decreasing values of momentum

thickness Reynolds number, defined as:

$$R_\theta = \sin\lambda[.1425K+.405][(r*R/ft)/(\cos\lambda*(1+t/c))]^{1/2}$$

using the geometric approximation method of ref. 10. The non-dimensional leading edge suction velocity K for the actual test conditions varied from -0.15 to -0.19 with C_q = -0.00035 where C_q is averaged over the leading edge perforated and non-perforated area of flutes 1 and 2 (Table 2). The amount of suction used here reduces the momentum thickness Reynolds number at the attachment line about 7 percent as compared to the zero suction case (fig. 11). Figures 10-1 and 10-2 show more laminar flow outboard than inboard. This is due to the smaller outboard nose radius and the resulting larger leading edge velocity gradient, which lowers the momentum thickness Reynolds number. The data of figure 10 clearly show the need to provide the test article with protection from turbulence contamination coming off the inboard wing. Without the bump and using suction, laminar flow could not be obtained over the entire test article at any flight condition. In figure 10, the suction coefficient for flute 9 was zero for the 'bump off' flight due to a malfunctioning valve. However, close examination of the data showed no impact on the results.

Figure 12 summarizes the experimental attachment line momentum thickness Reynolds number without the bump at a wide variety of flight conditions, again using the method of reference 10 to calculate R_θ. These data indicate that for R_θ greater than about 94, leading edge turbulence contamination causes transition. These data show remarkable agreement with the results of ref. 10. Redecker (ref. 15) suggests that the presence of the fuselage may effectively add about two degrees of sweep to the leading edge for the VFW-614 aircraft studied. If the R_θ calculations are repeated using an effective sweep angle of 32 degrees, R_θ would increase approximately 7 percent so that the critical R_θ for transition would be about 100.

The effect of suction on the attachment line boundary layer with and without the Gaster bump is shown in Figure 13 for M≈0.70 and R/ft = 1.52-1.64 x E06. Without the bump and without suction on the attachment line, very little laminar flow is obtained (fig. 13-5). Without the bump, but with suction on the attachment line, laminar flow is obtained over most of the span of the test section except for the most inboard location (fig. 13-4). With the bump, laminar flow is obtained with or without suction on the attachment line (flute 1, fig. 13-1,2).

Suction

Typical suction distributions are given in figure 10. Nominal suction levels were representative of that required in the leading edge of an LFC wing with nearly full chord laminar flow; that is, more suction than required for laminar flow to the front spar. Nominal suction requirements were defined in this way in the design of the wing so that the wing suction ducting volume would represent future transport applications with extensive laminar flow. High initial suction levels were required to control crossflow at the leading edge. Beyond S/C = 0.05, a lower level of C_q was maintained to the front spar, again to represent the suction distribution required in a more extensive laminar flow application.

Figure 14 presents results obtained with nominal suction (planforms 1,2,3) and with all suction blocked (planforms 4,5,6) by sealing the perforations with wax. With nominal suction (and with the bump), laminar flow is achieved on the test article. Without suction on flutes 1-15 (and with the bump), very little laminar flow was obtained at any flight condition studied due to the adverse effects of crossflow and transition occured between 0.5 and 2.1 percent chord.

Further suction experiments were made at the 0.775/29000 foot test point with suction levels increased (fig. 15) in gradual increments relative to nominal. (Note the change in the vertical scale.) The relative level of suction applied can be obtained from the inset number given in the suction coefficient section of figure 15. Oversuction of approximately 130 percent relative to nominal (fig. 15-6 vs fig. 15-2) did not result in any loss of laminar flow despite the much thinner boundary layer (fig. 16) and increased sensitivity to surface roughness. The possibility exists, however, that increased disturbances from the high suction flow through the perforations may grow downstream of the front spar and move transition forward at large length Reynolds numbers.

Early vs Later Leading Edge Suction

Suction location is known to strongly influence laminar flow. Early suction can be used to damp crossflow disturbance growth before it amplifies and causes transition. Theoretical investigations of both two and three dimensional flows (refs. 16-18) have shown that suction requirements for laminar flow can be minimized if suction is applied early where disturbances are small rather than farther downstream after the disturbances have amplified. Wind tunnel experiments (refs. 19-20) have confirmed the two-dimensional theoretical results (but not the three-dimensional case). There are, however, no flight data available on this subject on actual wing surfaces where measurements are concentrated in the leading edge region. The test article configuration described herein enabled such measurements. Questions studied include the effect of suction in the leading edge region where crossflow is dominant and also include the effect of suction closer to the front

spar where the relatively flat pressure gradient tends to damp crossflow but promote Tollmien-Schlichting disturbance growth.

Comparison of early vs later leading edge suction was accomplished at the 0.775/29000 test point by sealing flutes spanwise at either the trailing edge or leading edge of the test article. Results are presented where suction is progressively added from either the rear or forward direction. Later suction (fig. 17) results in a relatively thick leading edge boundary layer as compared with early suction (fig. 18). These data clearly show the importance of suction location in controlling crossflow; transition occurs near the leading edge when suction is applied only to flutes 6-15 (fig. 17-2) or flutes 5-15 (fig. 17-3). With suction at flute 4 (fig. 17-4), laminar flow is suddenly obtained to the front spar! Adding suction from the front direction (fig. 18) shows that laminar flow was not generally obtained to the front spar until suction was used on flutes 1-6. The localized loss of laminar flow, probably due to the slight adverse gradient near the front spar caused by the Pitot rake installation, was eliminated with further suction through flute 15. Data from M=0.775 to 0.70 are compared in figure 19 where suction is applied to flutes 1-5 vs 5-15. Overall suction up to the transition point is maintained at about the same level as shown at Mach=0.775 in fig. 19-1 vs 19-4, and early suction yields a longer run of laminar flow. The darkened area in the suction coefficient figures represents suction used past the average transition point. At Mach=0.75 (figure 19-2 vs 19-5), more laminar flow is also obtained with early suction than with later suction despite using more suction with the later suction case. No clear result is evident in comparing the $M = 0.70$ data of fig. 19-3 vs 19-6 although the later suction configuration had considerably more suction.

Suction Summary

The experimental results shown here indicate that suction control of boundary layer disturbance growth, while often successful, is not a cure-all for all disturbance growth control. Suction can only do so much to maintain laminar flow. Proper design, fabrication, and maintainence of laminar flow control wing surfaces are still the most important factors in the practical application of laminar flow control technology.

Comparison With Theory

The measured pressure distributions at the test point 0.775/29000, as shown in figs. 15, 17, and 18, are represented by the curve-fit shown in figure 9. This single pressure distribution was utilized to compute the mean flow for all suction configurations studied using the swept-wing laminar boundary layer computer code of ref. 22. The actual suction rates through the perforated strips were area-averaged over the entire flute area including the perforations blocked by the support structure in order to model a continuous suction distribution (Table 2). Boundary layer stability calculations were made using an improved linear stability theory which accounts for streamline and surface curvature and compressibility (ref. 21) to determine the effect of suction location and magnitude on disturbance growth as indicated by the N-factor. The maximum amplification option of the code (ref. 23) was used to calculate the N-factor. The stability calculations for the 0.775/29000 test point are presented in figures 20-23 and the results are summarized in Table 3.

For the case of nominal suction (laminar flow to the front spar, figure 14-1), N-factors computed with and without the curvature terms in the linear stability equations are presented in figure 20 for 6000 Hz. and for 0 Hz. A range of frequencies were computed to determine the frequency which produced the largest N-factor at the transition location or at the front spar, and disturbances at 6000 Hz. were found to be the most amplified (fig. 20). The N-factor computed without curvature at 6000 Hz. reaches the currently assumed critical value for transition of 9 (based on previous correlations) at about 3 percent chord although transition did not occur until 13 percent chord. When the curvature terms are included in the calculation, the N-factor for the most amplified frequency is well below this assumed critical value and in fact shows that the boundary layer is stable from about 5 percent chord back to the front spar. This result emphasizes the importance of including the dominant physical effects (body and streamline curvature, compressibility, etc.) in the stability calculations.

A comparison of the N-factors (including the effects of curvature) for the case of no suction and the case of nominal suction at 0.775/29000 is presented in figure 21. In the case of no suction, laminar boundary layer transition occurs at $X/C = 0.021$ which is an average value determined from the experimental measurements (figure 14-4). The wave orientation angle, ψ, and wavelength to boundary layer thickness ratio, λ/δ, of the most amplified disturbance at the transition location were computed as about 84 degrees and 4.3, respectively. These are values typical of crossflow disturbances, indicating that transition is due to the growth of highly amplified crossflow disturbances. The N-factor at transition was about 8.4 for the case of no suction at the most amplified frequency. As can be seen in figure 21, the effect of suction on the boundary layer reduces the amplification rates (and hence the N-factor) of the crossflow vortices well below the critical value of about 9, and laminar flow is achieved to the front spar (as indicated from the experimental

measurements shown in figure 14-1).

The effect of suction location and magnitude on the stability of the boundary layer at 0.775/29000 is presented in figure 22 and 23. In figure 22, N-factor calculations as a function of X/C are shown for the cases of no suction and suction on flutes 8-15, 7-15, 6-15, 5-15, and 4-15 (later suction) at a frequency of 6000 Hz. which is (or very close to) the most amplified frequency for each suction configuration. (See figure 17 for experimentally determined transition locations). In each case, the growth of crossflow disturbances in the laminar boundary layer is significant, causing transition in all cases except for the case of suction on flutes 4-15. The N-factor at transition for the other suction configurations is between about 10.0 and 10.5 (Table 3). The maximum N-factor for the case of suction on flutes 4-15 does not exceed 8.5 and, as mentioned, the experiment shows laminar flow to the front spar. For suction on flutes 8-15, suction does not influence transition since all the suction is aft of the transition location.

In figure 23, the N-factor calculations for the cases referred to as early suction are presented along with the case of no suction. With suction applied to flutes 1 and 2, transition was experimentally determined to occur at $X/C = 0.035$ (see figure 18), and according to the stability theory, transition is dominated by the growth of highly amplified crossflow disturbances with the wave orientation about 84 degrees at transition. The N-factor at transition is about 7.6; lower than the N-factors found for the later suction data discussed earlier. As more suction is added, transition moves farther back along the chord. For the cases of suction on flutes 1-5, 1-6, and 1-7, the stability theory predicts that crossflow-like disturbances are most amplified to about 4 percent chord followed by a region where TS waves are most amplified (fig. 23). In fact, for the case of suction on flutes 1-5, the wave orientation angle was 45.5 degrees and the wavelength to boundary layer thickness ratio was 12.5, values typical of TS waves at the transition location of 9.5 percent chord. All the transition correlations are summarized in Table 3.

The crossflow Reynolds number has been used in the past to correlate leading-edge transition data for flows with favorable chordwise pressure gradients (ref. 14). The crossflow Reynolds number at transition as a function of leading edge sweep angle is presented in figure 24 for a number of wind tunnel and flight investigations. The present data agrees very well with the investigation of ref. 14 which determined the critical value of crossflow Reynolds was about 325.

Summary and Conclusions

Laminar flow research with suction on the leading edge of a swept wing was accomplished for the first time since the X-21 flights ended in 1965. Achievement of laminar flow on the test article surface required both a bump on the inboard leading edge to negate the turbulent boundary layer propagating along the attachment line from the fuselage, and suction on the test article at all test conditions. Generally, 100 percent laminar flow was obtained to the front spar with nominal suction at most test conditions. Suction was also increased 130 percent over the nominal suction and laminar flow was maintained to the front spar despite the thinner boundary layer. At the 0.775/29000 test point, early suction on the leading edge yielded more laminar flow than did later suction for the same amount of overall suction.

Theoretical predictions were made using a state-of-the-art linear stability theory which accounts for body and streamline curvature and compressibility as suction location and magnitude varied. N-factor correlations with transition location were made at a Mach number/altitude combination of 0.775/29000. These calculations showed that the body and streamline curvature effects on the 30 degree swept wing used here reduced disturbance amplification and N-factors by as much as about 60 percent for some flight conditions. It was shown that N-factors at transition varied from about 7.5 to 10.5, and that early suction resulted in N-factors at transition lower than N-factors associated with later suction.

References

1. Douglas Aircraft Company Staff: Laminar Flow Control Leading Edge Flight Test Article Development. NASA CR-172137, 1984.
2. Fisher, D.F.; and Fischer, M.C.: The Development Flight Tests of the JetStar LFC Leading Edge Flight Experiment. NASA CP 2487, pp. 117-140, 1987.
3. Davis, R.E.; Maddalon, D.V.; Wagner, R.D.; Fisher, D. F.; and Young, R.: Performance of Laminar Flow Leading Edge Test Articles and Cloud Detection Instruments During the NASA Left Program. NASA TP 2888, 1989.
4. Powell, A.G.; and Varner, L.D.: The Right Wing of the LEFT Airplane. NASA CP 2487, pp. 141-161, 1987.
5. Maddalon, D.V.; Fisher D.F.; Jennett, L.A.; and Fischer, M.C.: Simulated Airline Service Experience with Laminar Flow Control Leading-Edge Systems. NASA CP 2487, pp. 195-218, 1987.
6. Wagner, R.D.; Maddalon, D.V.; and Fisher, D.F.: Laminar Flow Control Leading Edge Systems in Simulated Airline Service. ICAS-88-3.7.4. Jerusalem, Israel. 1988.
7. Petley, D. H.; Alexander, W. Jr.; Wright, A. S. Jr.; and Vallas, M.: Calibration of Sonic Valves for the

Laminar Flow Control, Leading-Edge Flight Test. NASA TP 2423, 1989.

8. Pfenninger, W.: Some Results from the X-21 Program. Part I - Flow- Phenomena at the Leading Edge of Swept Wings. From Agardograph 97, Part IV - Recent Developments in Boundary Layer Research, 1965.
9. Bacon, J. W. Jr.; and Pfenninger, W.: Transition Experiments at the Front Attachment Line of a 45 deg. Swept Wing With a Blunt Leading Edge. AF FDL TR 67-33, 1967.
10. Pfenninger, W.: Laminar Flow Control Laminarization. AGARD-R-654, June 1977.
11. Gaster, M.: On the Flow Along Swept Leading Edges. The Aeronautical Quarterly, Vol. XVIII, pp. 165-184, May 1967.
12. Gaster, M.: A Simple Device for Preventing Turbulent Contamination on Swept Leading Edges. Journal of the Royal Aeronautical Society, Vol. 69, pg. 788, 1965.
13. Cebeci, T. : Attachment Line Flow on an Infinite Swept Wing. AIAA Journal, Vol. 12, No. 2, February 1974, pp. 242-245.
14. Poll, D. I. A.: Some Aspects of the Flow Near a Swept Attachment Line With a Particular Reference to Boundary Layer Transition. Cranfield Institute of Technology, CoA Report No. 7805, 1978.
15. Redeker, G. and Wichmann, G.: Forward Sweep– A Favorable Concept for a Laminar Flow Wing. AIAA-88-4418, 1988.
16. Nayfeh, A.H.; Reed, H.L.; and Ragab, S.A.: Flow Over Plates With Suction Through Porous Strips. AIAA Journal, Vol. 20, No. 5, pp. 587-588, May 1982.
17. Reed, H.L.; and Nayfeh, A.H.: Numerical Pertubation Techniques for Stability of Flat Plat Boundary Layers with Suction. AIAA Journal, Vol. 24, No. 2, pp. 208-214.
18. Nayfeh, A.H.; and Reed, H.L.: Stability of Flow over Axisymmetric Bodies with Porous Suction Strips. Physics of Fluids, Vol. 28, No. 10, pp. 2290-2998, October 1985.
19. Reynolds, G. A.; and Saric, W.S.: Experiments on the Stability of the Flat Plate Boundary Layer with Suction. AIAA Journal, Vol. 24, No. 2, pp. 202-207, 1986.
20. Saric, W.S., and Reed, H.L.: Effect of Suction and Weak Mass Injection on Boundary Layer Transition. AIAA Journal, Vol. 24, No. 3, pp. 383-389,1986.
21. Collier, F.S., Jr.: Curvature Effects on the Stability of Three-Dimensional Laminar Boundary Layers. Ph. D. Dissertation, Virginia Polytechnic Institute and State University, May 1988.
22. Kaups, K. and Cebeci, T.: Compressible Laminar Boundary Layers With Suction on Swept and Tapered Wings. J. Aircraft, Vol. 14, pp. 661-667, July 1977.
23. Malik, M.R.: Cosal-A Black Box Compressible Stability Analysis Code for Transition Prediction in Three-Dimensional Boundary Layers. NASA CR-165925, 1982.

Table 1 Perforated test article midspan flute locations

	FLUTE	X/C SUCTION CENTERLINE	S/C SUCTION CENTERLINE
LEADING EDGE	1	.0021	.0068
	2	.0004	.0006
	3	.0031	.0083
	4	.0082	.0163
	5	.0153	.0255
	6	.0244	.0359
	7	.0347	.0459
	8	.0450	.0590
	9	.0557	.0703
	10	.0664	.0818
	11	.0770	.0930
	12	.0879	.1043
	13	.0987	.1156
	14	.1099	.1269
	15	.1200	.1382

Table 2 Suction location and suction coefficient used in stability calculations (0.775/29000).

Flute	Suction Begins (X/C)	Suction Ends (X/C)	Perf. Area / Total Area	Nominal $Cq_{meas.}$ Midspan	** Nominal Cq Midspan
1	.001700 *	.000186 *	.466	-.000706	-.000329
2	.000186 *	.001290	.484	-.000737	-.000357
3	.001290	.005262	.612	-.000648	-.000397
4	.005262	.011450	.624	-.000639	-.000399
5	.011450	.019629	.616	-.000672	-.000414
6	.019629	.029387	.609	-.000652	-.000397
7	.029387	.039905	.626	-.000549	-.000344
8	.039905	.050271	.615	-.000222	-.000137
9	.050271	.061043	.618	-.000296	-.000183
10	.061043	.071680	.619	-.000081	-.000050
11	.071680	.082417	.622	-.000113	-.000070
12	.082417	.093339	.612	-.000123	-.000075
13	.093339	.104146	.592	-.000195	-.000115
14	.104146	.115021	.647	-.000647	-.000210
15	.115021	.126000	.625	-.000625	-.000206
1-15 chordwise average	—	—	—	-.000391	-.000236

*Lower Surface

**Cq area averaged to include non-perforated area necessary to simulate continuous suction surface for boundary layer calculations

Table 3 Summary of N-factor correlations with transition locations at 0.775/29000.

Suction	$(X/C)_T$	N_{max}	N_{max} (0 Hz.)	R_{CF}	ψ (deg.)	λ/δ
None	2.1	8.4	5.1	317	83.9	4.3
8-15 on	3.9	10.6	5.7	350	82.2	4.6
7-15 on	3.9	10.4	5.7	350	82.9	4.5
6-15 on	4.2	10.0	5.6	na	83.2	4.4
5-15 on	6.5	9.9	5.4	na	82.4	4.6
1-2 on	3.5	7.6	5.1	340	82.3	4.6
1-5 on	9.5	7.8	stable	na	45.5	12.5
1-6 on	12.4	8.4	stable	na	54.8	12.6

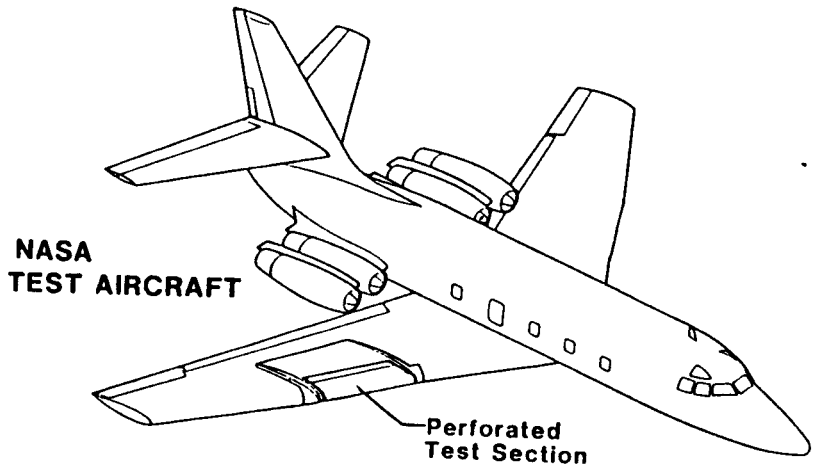

Figure 1 The NASA Laminar Flow Control Flight Test aircraft.

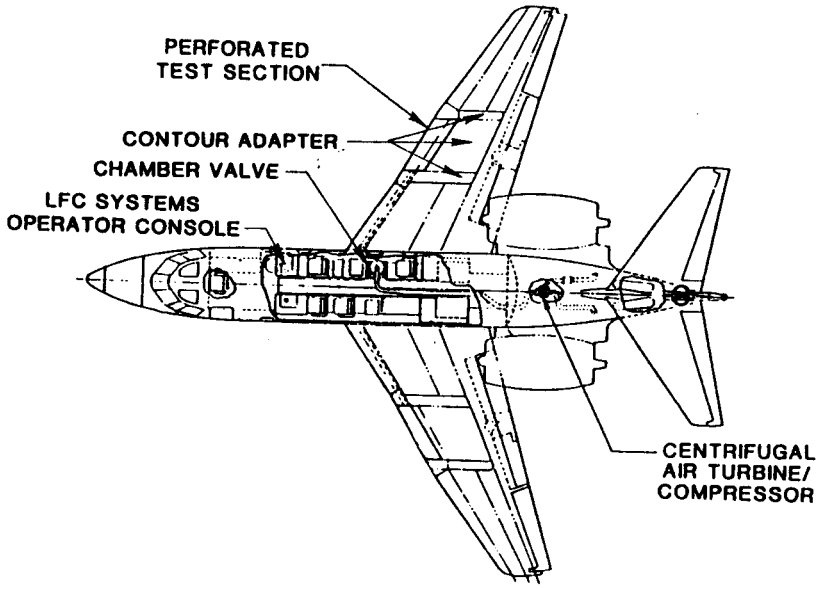

Figure 2 Suction leading-edge test aircraft.

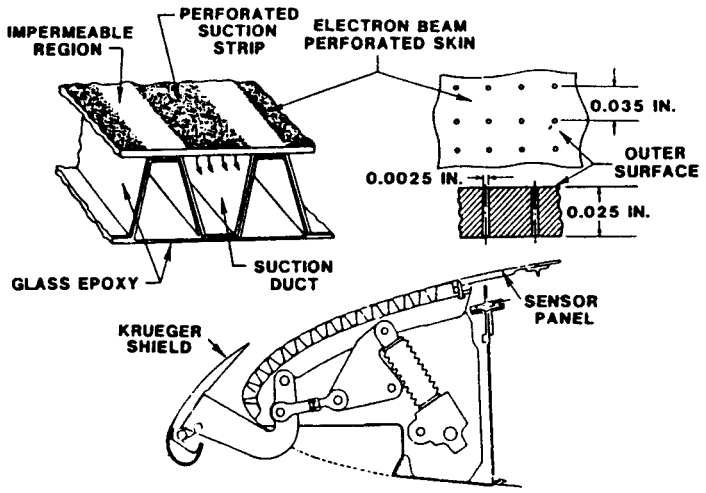

Figure 3 Cross-section of the perforated test article.

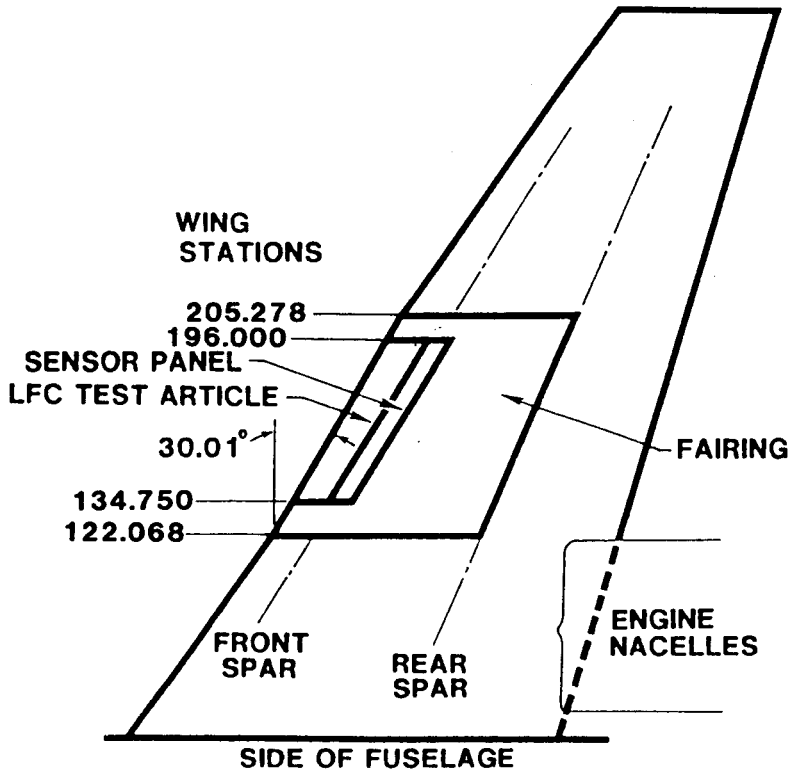

Figure 4 Planform of the leading-edge test article.

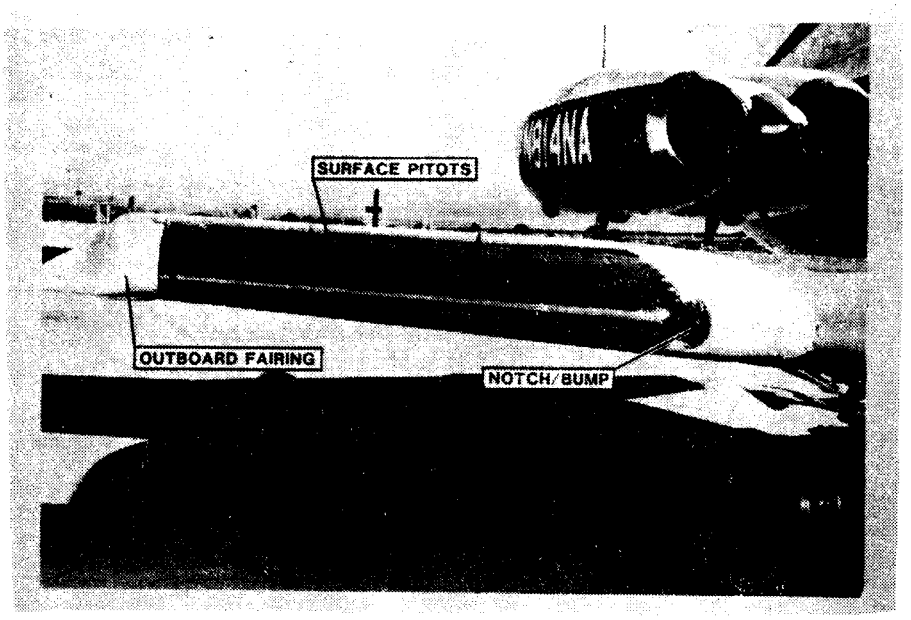

Figure 5 Perforated test article installed on test aircraft.

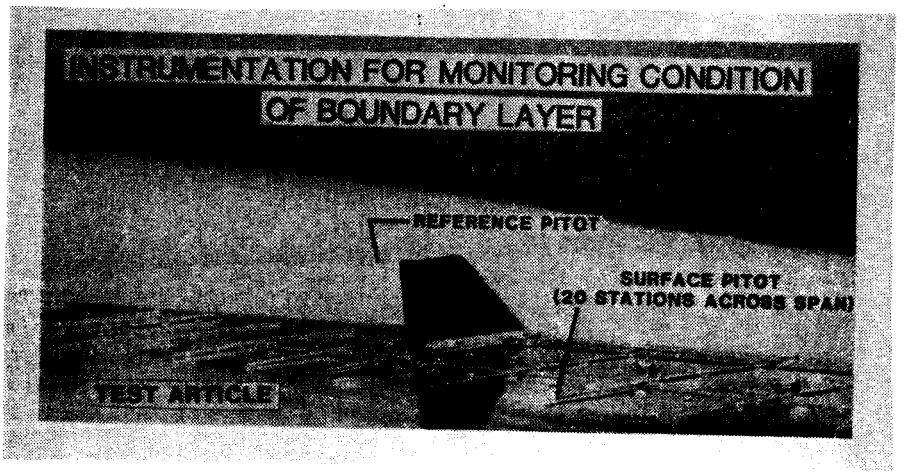

Figure 6 Transition sensing intrumentation at front spar.

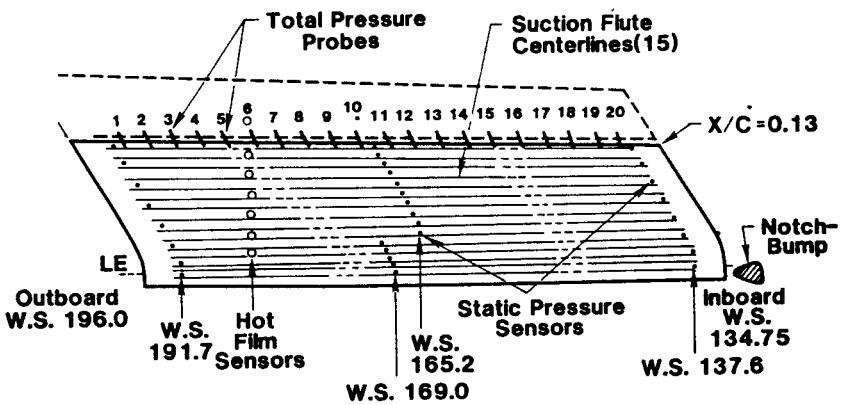

Figure 7 Perforated test article surface instrumentation.

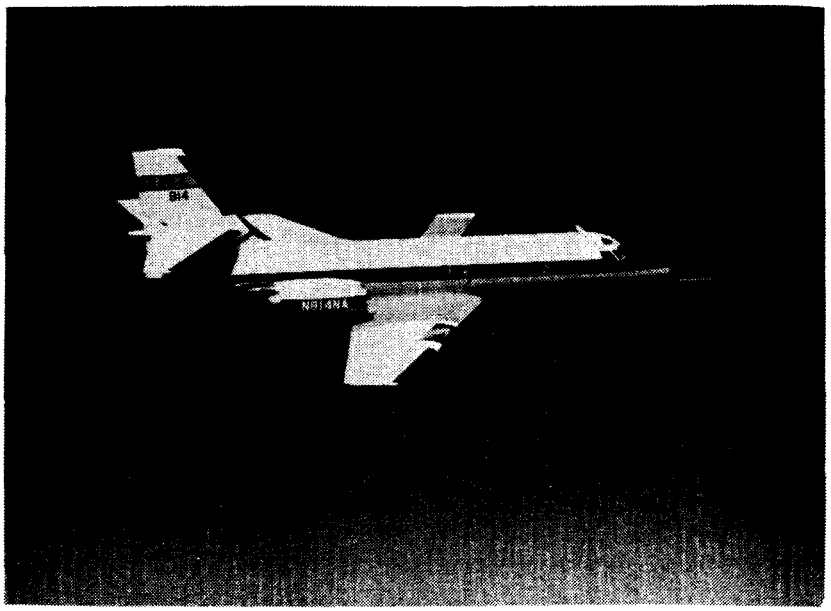

Figure 8 Test aircraft in flight.

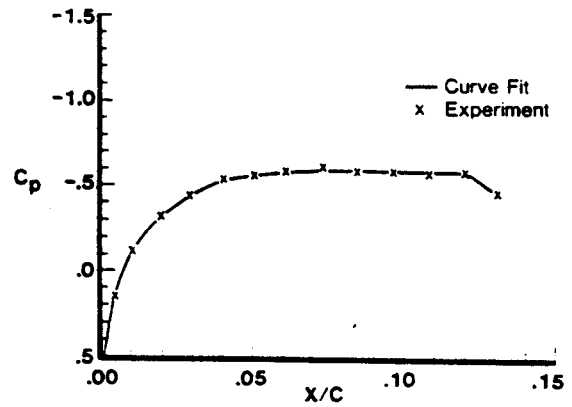

Figure 9 Pressure coefficient distribution.

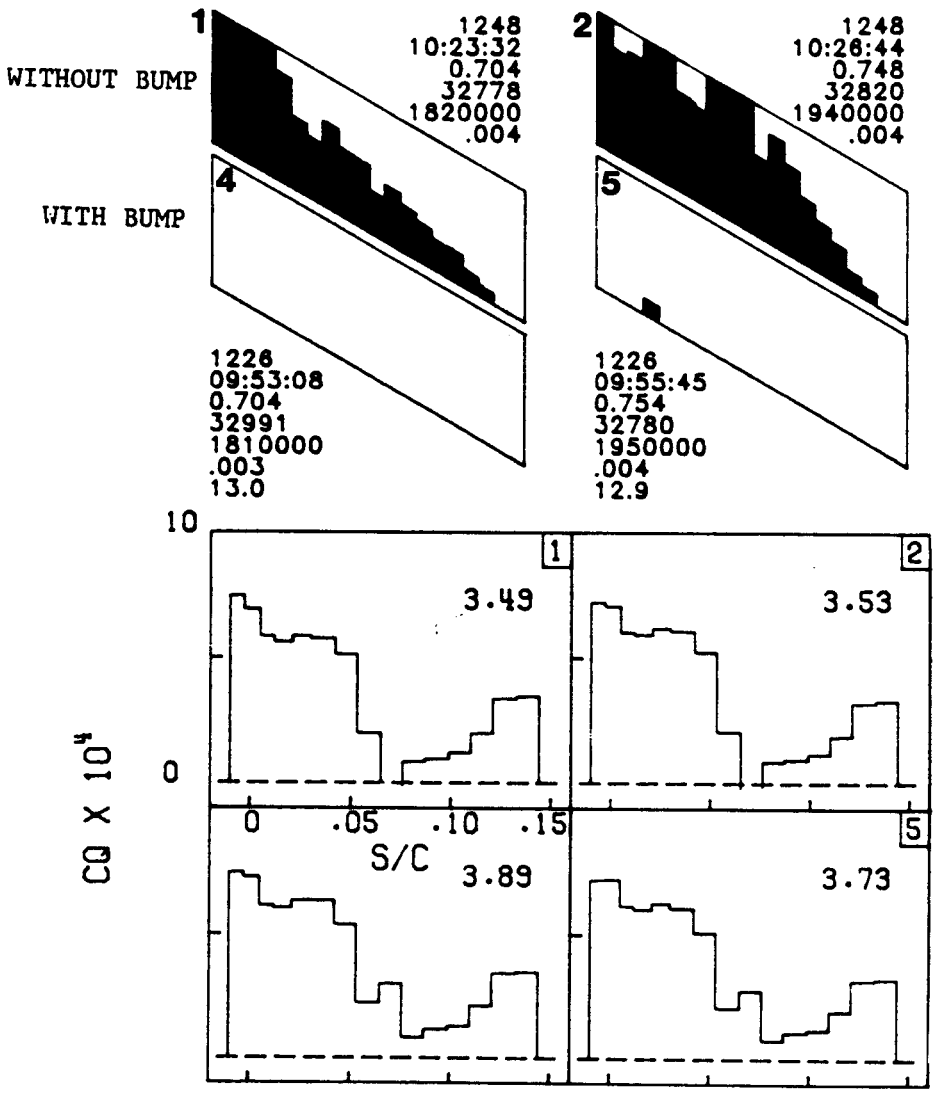

Figure 10 Effect of bump on leading-edge contamination at varying Reynolds numbers.

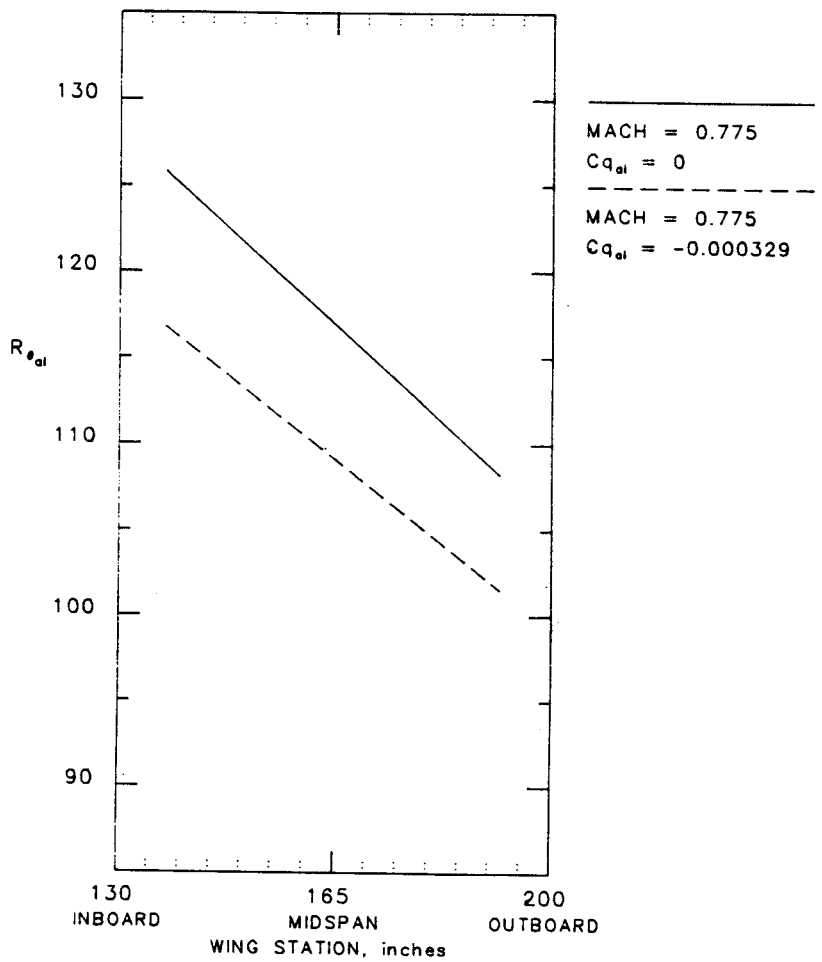

Figure 11 Experimental attachment line momentum thickness Reynolds numbers versus span.

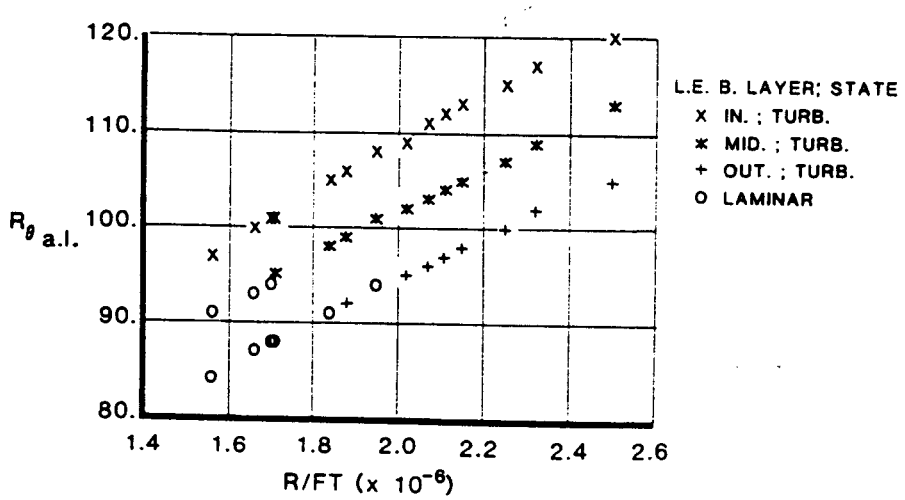

Figure 12 Experimental attachment line momentum thickness Reynolds number without bump.

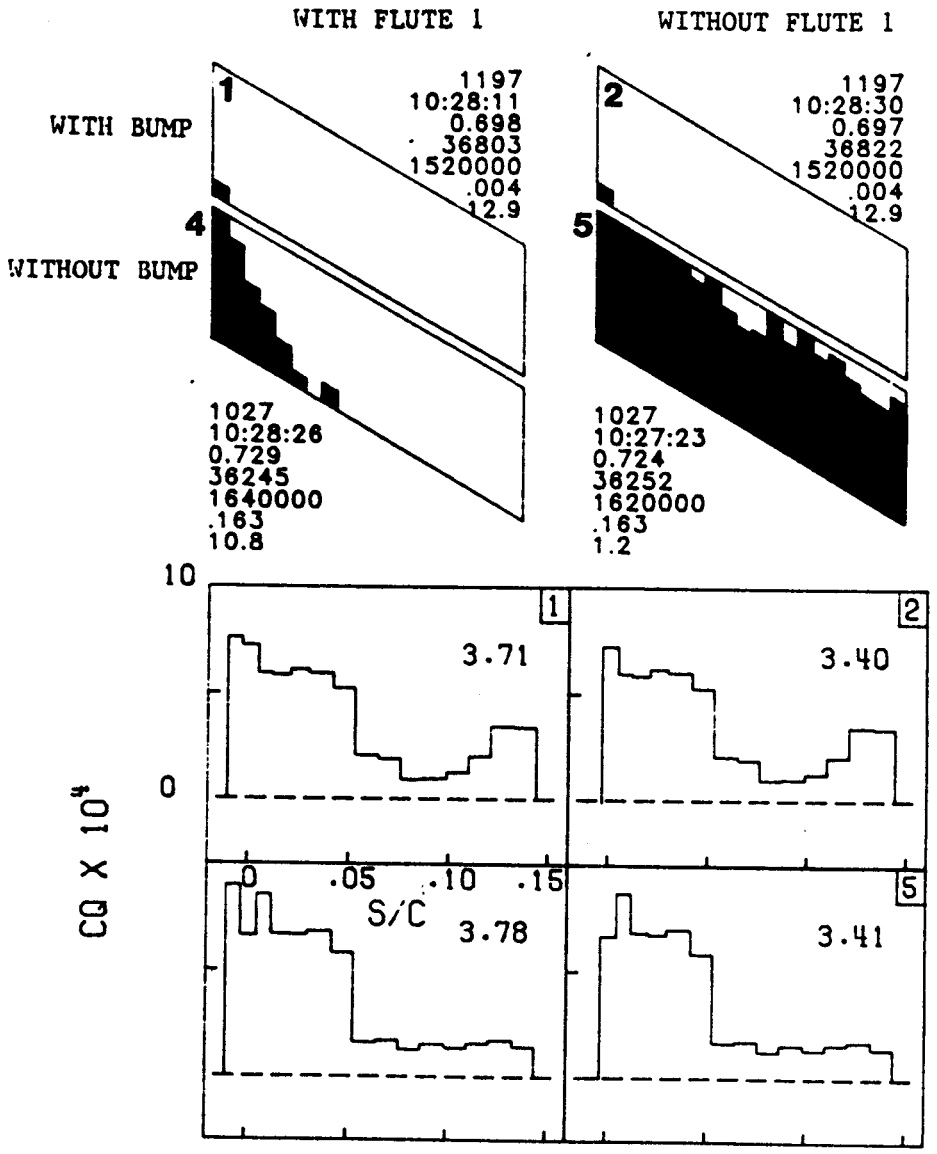

Figure 13 Effect of attachment line suction on leading-edge contamination with and without the bump.

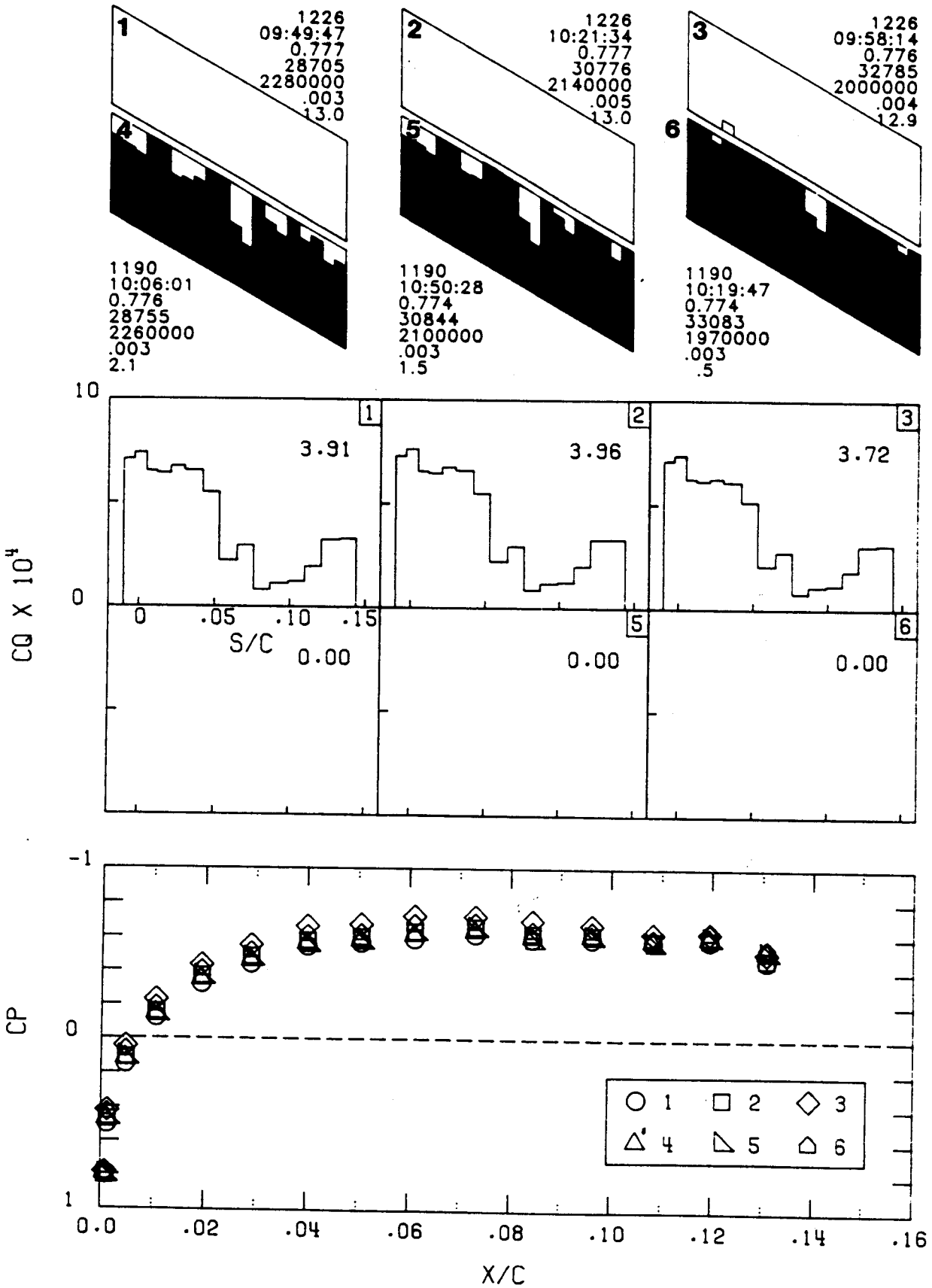

Figure 14 Effect of suction on transition location.

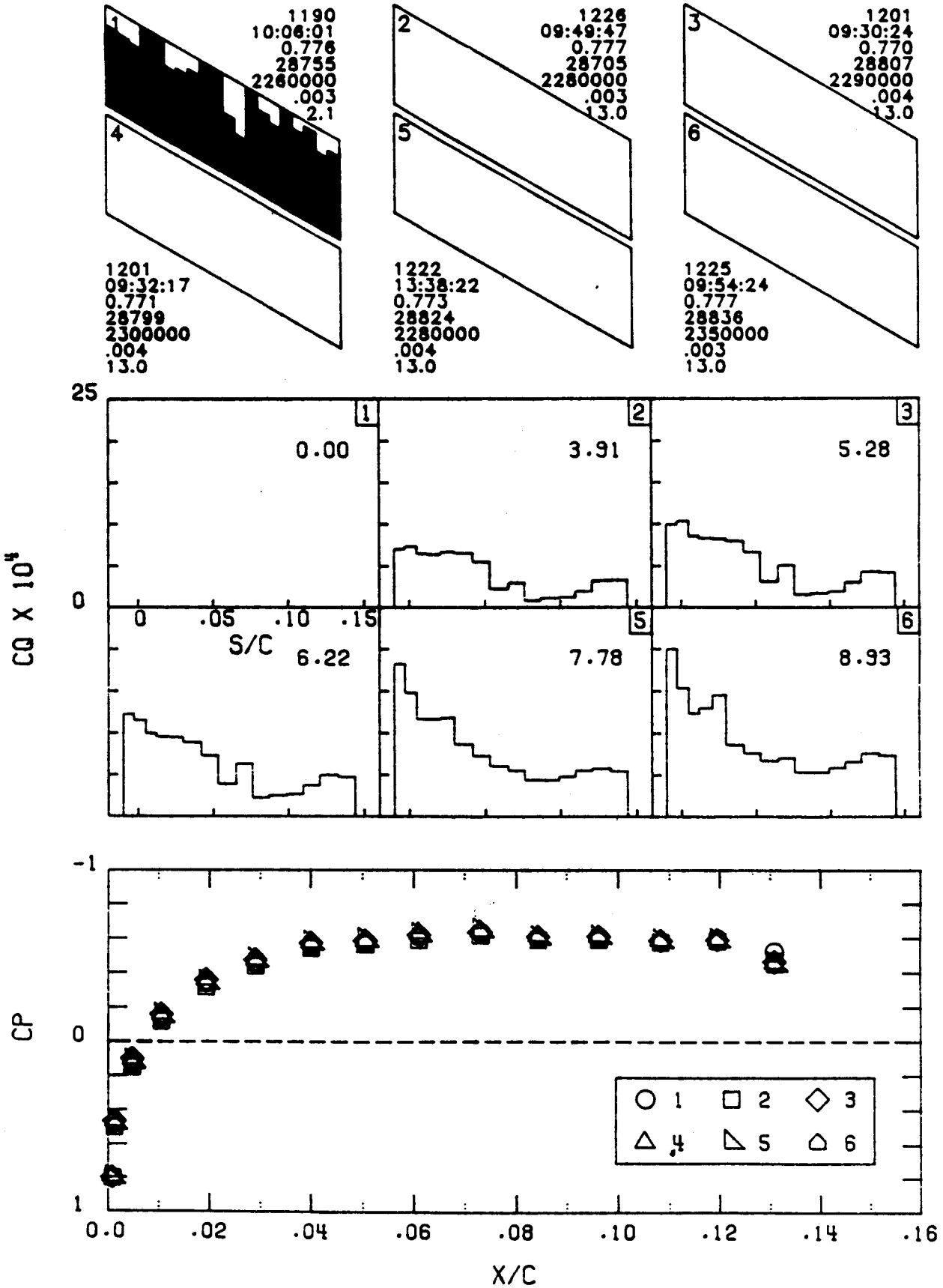

Figure 15 Effect of increased suction on laminar flow at the front spar.

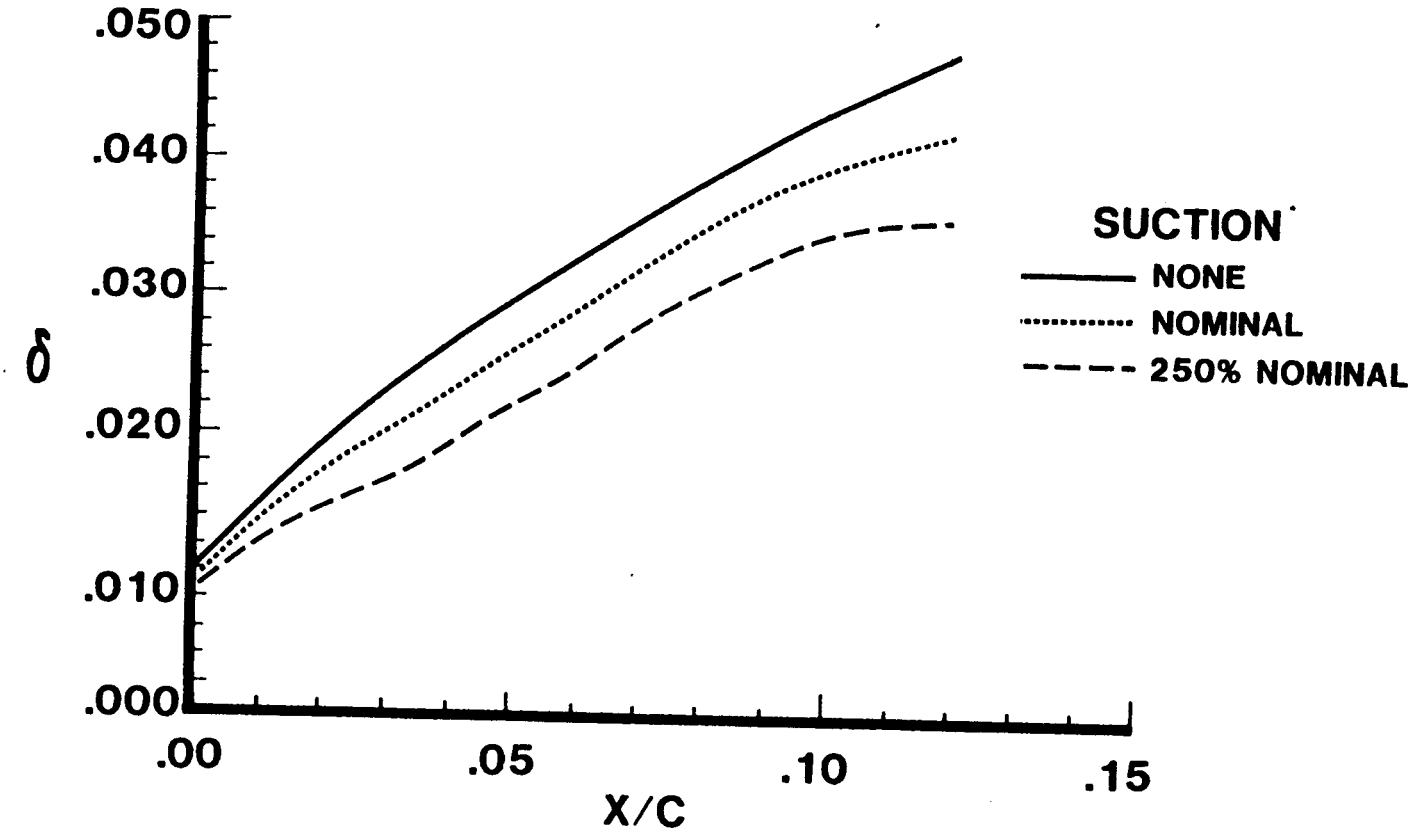

Figure 16 Effect of suction on boundary layer thickness at 0.775/29000.

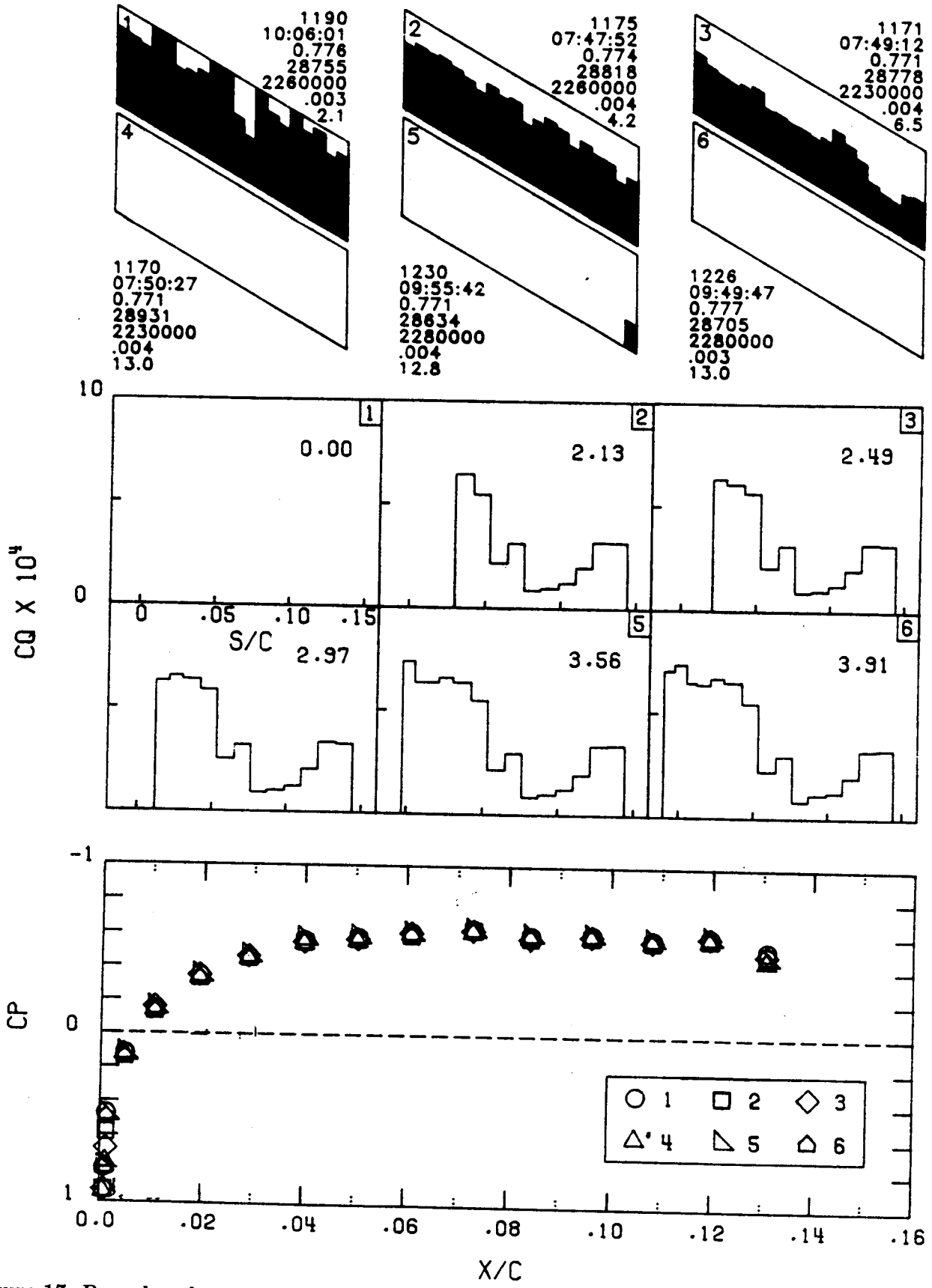

Figure 17 Boundary layer transition with later suction on flutes: none, 6-15, 5-15, 4-15, 2-15, and 1-15.

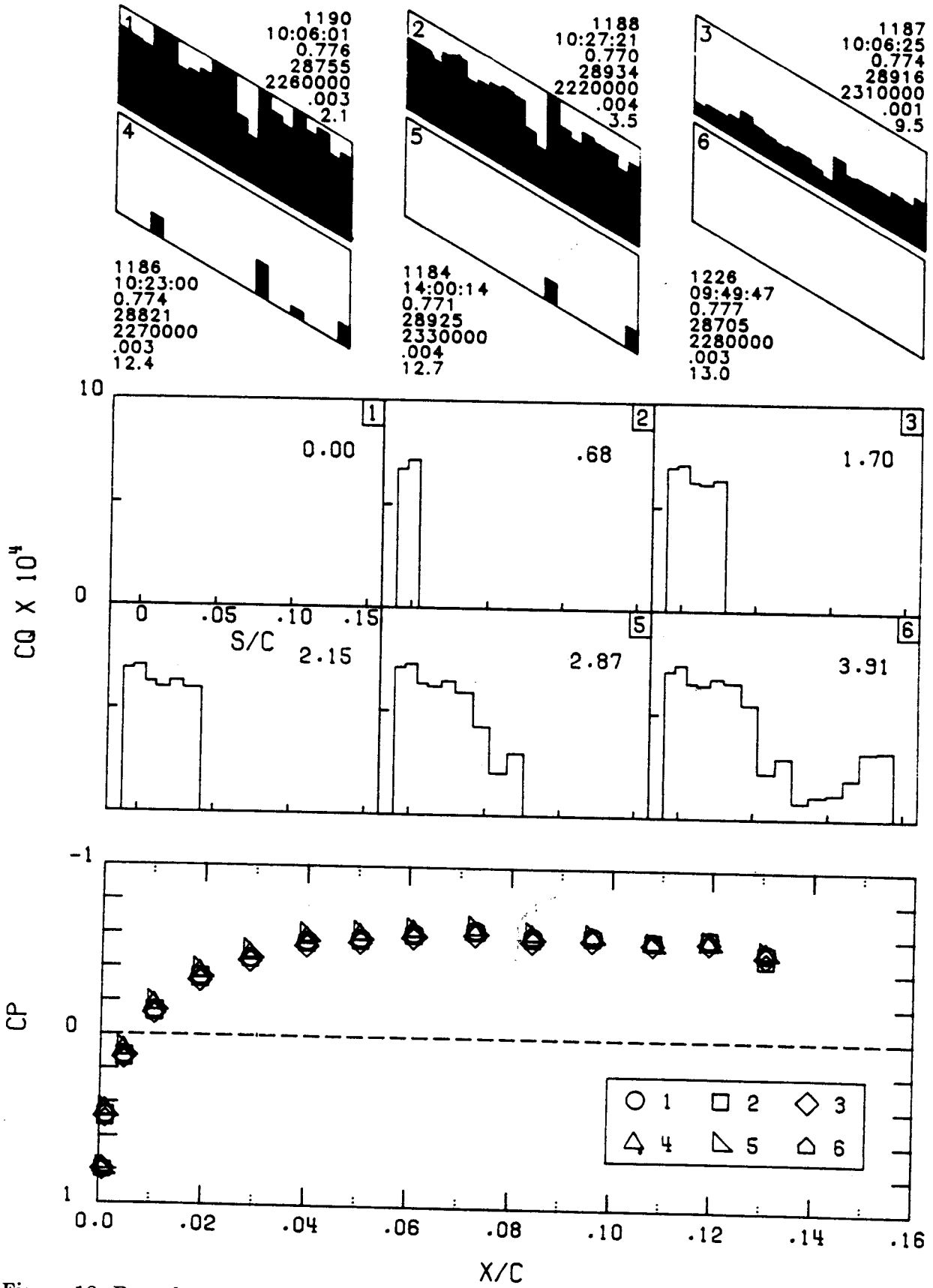

Figure 18 Boundary layer transition with early suction on flutes: none, 1-2, 1-5, 1-6, 1-9, and 1-15.

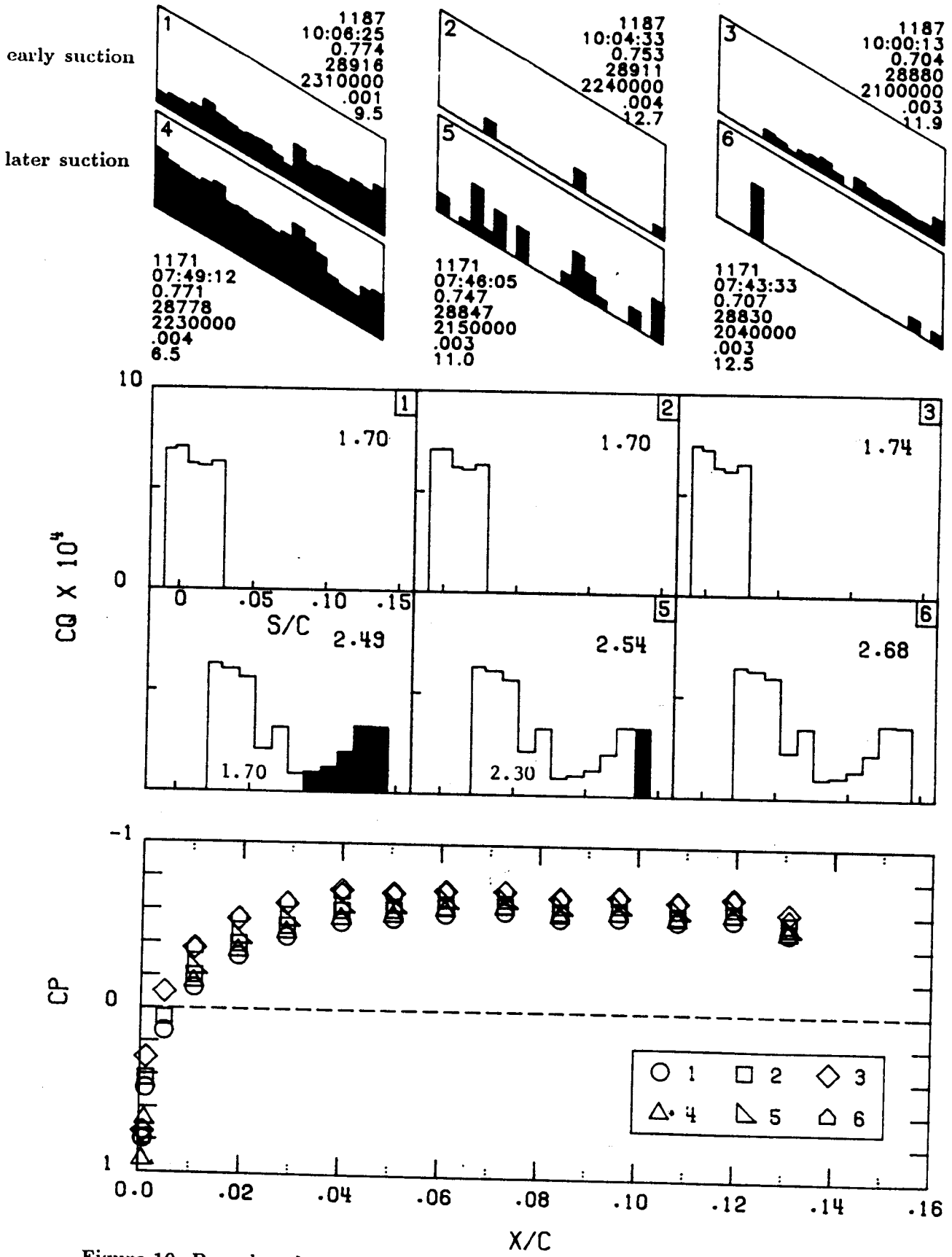

Figure 19 Boundary layer transition for early (flutes 1-5) versus later (flutes 5-15) suction.

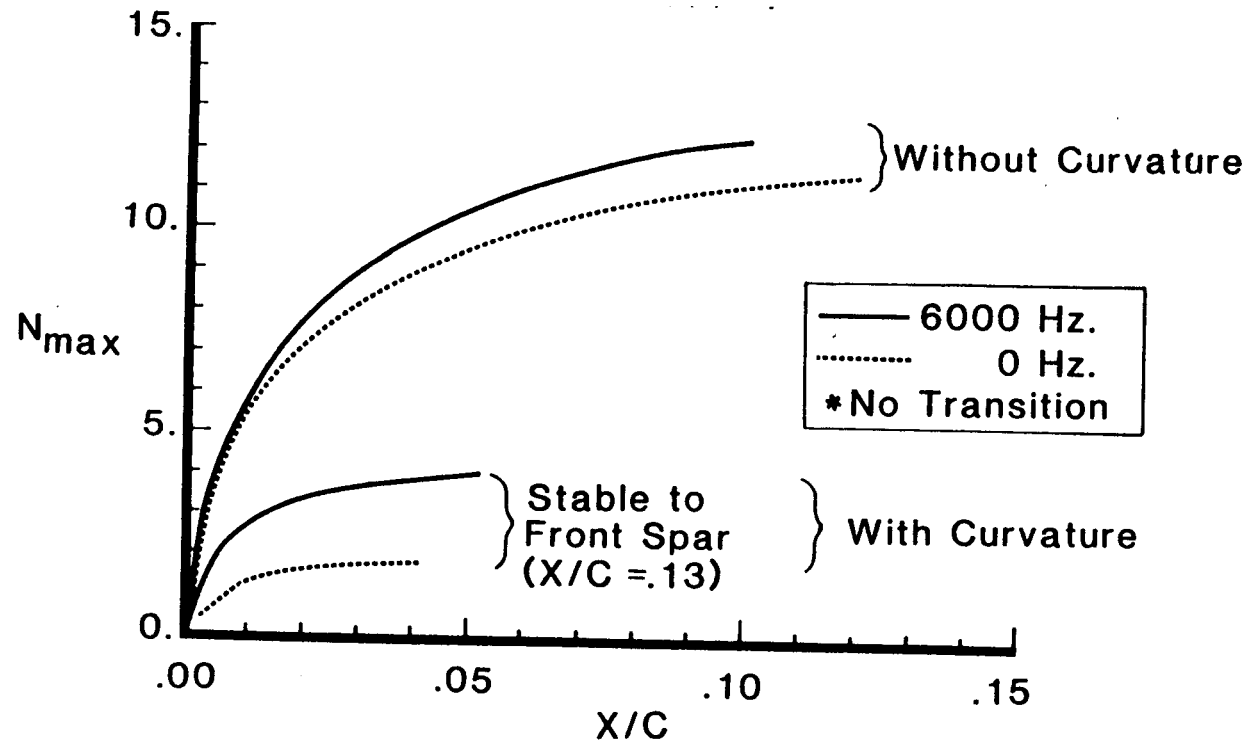

Figure 20 Effect of curvature on laminar boundary layer stability at M=0.775, 29000 ft. and nominal suction.

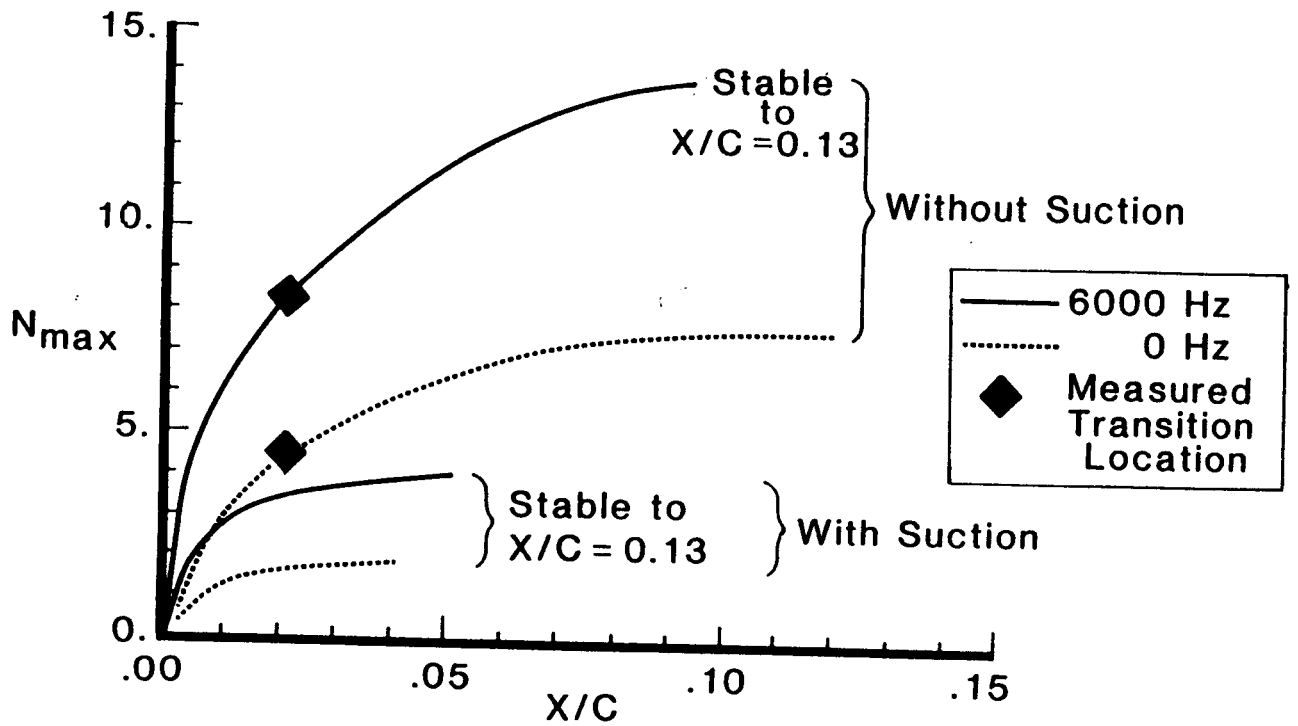

Figure 21 Effect of suction on laminar boundary layer stability at M=0.775, 29000 ft. including curvature effects.

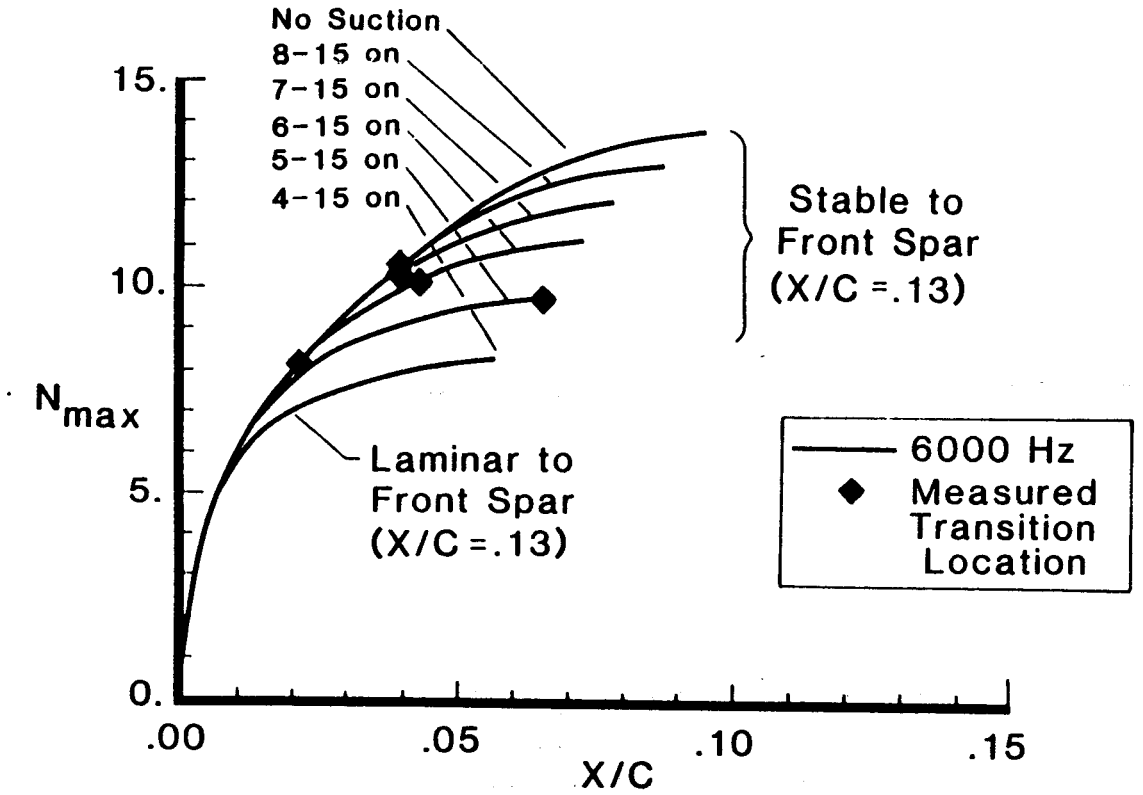

Figure 22 Effect of later suction on laminar boundary layer stability at M=0.775, 29000 ft. including curvature effects.

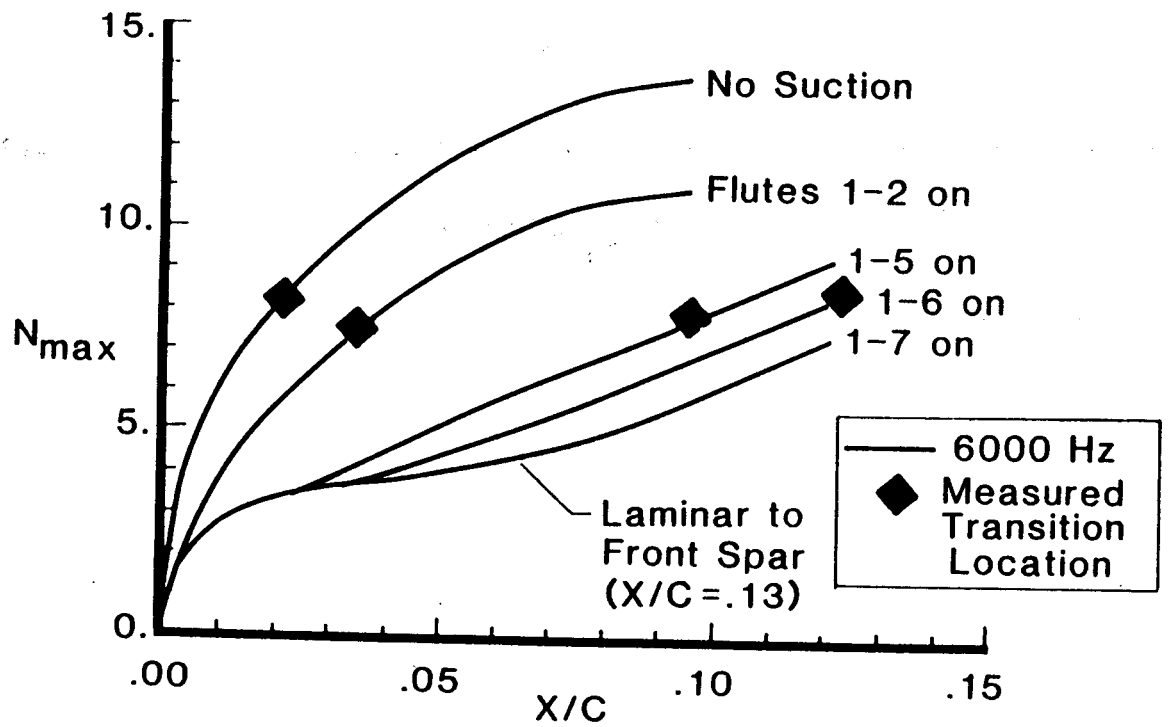

Figure 23 Effect of early suction on laminar boundary layer stability at M=0.775, 29000 ft. including curvature effects.

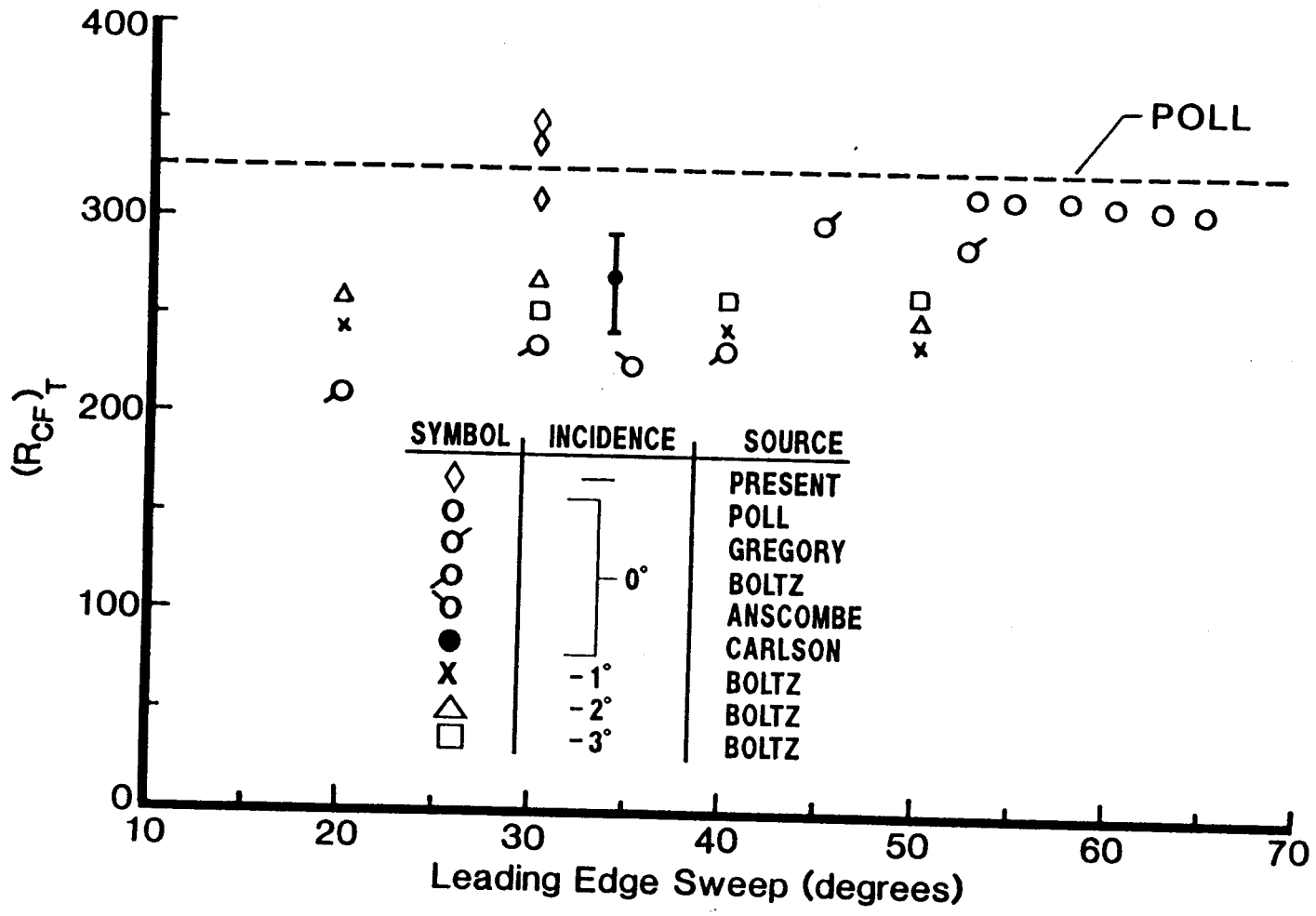

Figure 24 Crossflow Reynolds number for transition as a function of sweep.